



# Versatile Production of Multivariate, Hyperdimensional End Group and Main Chain Functionalized Polyolefins

Danyon M. Fischbach, Katharina A. Krstic, and Lawrence R. Sita\*

**Abstract:** The (stereoselective) living coordinative copolymerization of 1-alkenes with 4-aryl-1,6-heptadienes, in both the absence and presence of multiple equivalents of a reversible chain transfer agent, is established as a highly versatile strategy for production of multivariate hyperdimensional functionalized semi-crystalline or amorphous polyolefins that optionally possess either mono- or difunctionalized (telechelic) end-groups in combination with a programmable level of incorporation of orthogonal functional groups within the main-chain. The non-conjugated diene comonomers are readily obtained from a diverse range of aryl carboxaldehyde precursors through a one-step bis-allylation process. These results serve to provide a new platform for exploring the science and technology of a vast new landscape of functionalized classes of polyolefins that are now accessible in practical and scalable quantities.

**P**olyolefins, which are currently produced on an enormous global scale of 300 million tons per year, are the most successful synthetic material fashioned by humankind for the advancement of civilization.<sup>[1–3]</sup> First commercialized 70 years ago based on the seminal discoveries made by Ziegler and Natta, polyolefins are manufactured through the transition-metal-mediated coordinative polymerization and co-polymerization of a small set of industrially-relevant alkene monomers, and most significantly, ethene (E), propene (P), and a few additional higher-carbon-numbered linear and branched 1-alkenes, such as 1-butene (B), 1-hexene (H), and 4-methyl-1-pentene (4M1P) that are obtained from E and P through controlled dimerization or oligomerization.<sup>[4]</sup> Coordination polymerization converts these unsaturated 1-alkenes into the corresponding saturated hydrocarbon polyolefin products through a propagation mechanism involving  $\pi$ -complexation of the monomer to the active transition-metal species bearing a polymeryl

group, followed by 1,2-migratory insertion (1,2-MI) into the growing polymer chain. The supporting ligand environment about the transition-metal centre serves to control the relative rates of propagation vs termination, as well as enantioface selectivity of 1-alkene complexation to the metal center that then manifests as the stereochemical microstructure, or tacticity, of the polyolefin.<sup>[5]</sup> To date, a substantially large variety of different “grades” of polyolefins have traditionally been obtained through manipulation of differences in, for example: (1) molar mass, as defined by the number- and weight- average molar mass indices,  $M_n$  and  $M_w$ , respectively, (2) molar mass distribution (MMD), also known as dispersity,  $\mathcal{D}$  ( $=M_w/M_n$ ), (3) MMD profile, whether uni-, bi-, or multimodal, and (4) tacticity. In the case of copolymerization of two or more 1-alkene monomers, the number of grades expands even further through programmed variations in copolymer microstructure, such as alternating and random sequences of monomer repeat groups. With introduction of living coordination polymerization (LCP) and living coordinative chain transfer polymerization (LCCTP), the range of polyolefin copolymers has been extended even further with production of well-defined block copolymers through sequential addition of two or more olefin comonomers, including those that adopt nanostructured microphase-segregated morphologies in the condensed phase.<sup>[3a,6–8]</sup> Indeed, just based on these variables alone, it is safe to say that the full scope of *unfunctionalized* hydrocarbon-based polyolefins has still not been fully explored even with the present small set of monomers. As Figure 1 shows, upon introduction of physiochemically-active functional groups at either the chain ends, or as

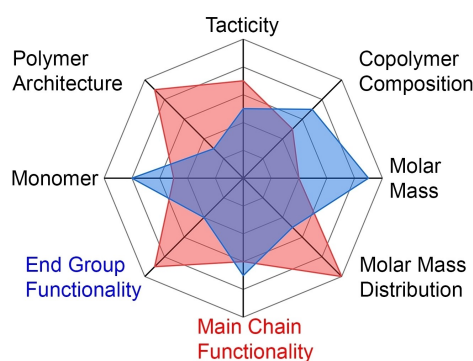
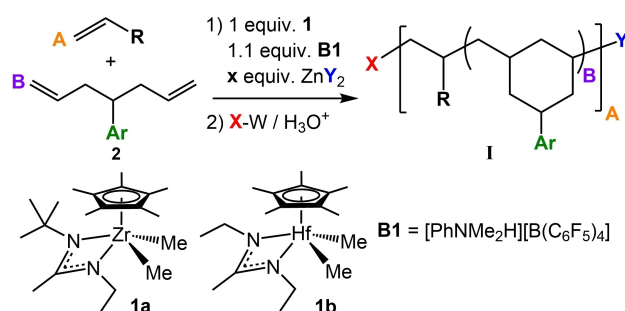


**Figure 1.** The multivariate, hyperdimensional landscape of next generation polyolefins showing traditional (black) and new variables (red and blue) governing structure/property/application relationships for two different hypothetical polyolefin materials.

[\*] D. M. Fischbach, K. A. Krstic, Prof. Dr. L. R. Sita  
Department of Chemistry and Biochemistry,  
University of Maryland  
20742 College Park, MD (USA)  
E-mail: lsita@umd.edu

© 2023 The Authors. Angewandte Chemie International Edition published by Wiley-VCH GmbH. This is an open access article under the terms of the Creative Commons Attribution Non-Commercial NoDerivs License, which permits use and distribution in any medium, provided the original work is properly cited, the use is non-commercial and no modifications or adaptations are made.

pendant groups off the main polymer chain, the extent of new categories of polyolefin materials now becomes truly unlimited.<sup>[9]</sup> In the face of such complexity, it is imperative to develop new paradigms that can be used to strategically access a large and diverse range of subclasses of new functionalized polyolefins in a “one catalyst—many materials” programmed fashion, rather than relying on an Edisonian approach that requires the synthesis and screening of large libraries of transition-metal complexes and polymerization conditions in order to map out structure/property/technological application relationships. Here, past efforts to introduce chemical functionality into polyolefins have largely been based on the design and synthesis of functionalized 1-alkene monomers that require protecting groups on the reactive elements in order to establish compatibility with the highly electrophilic character of early transition-metal coordination catalysts, followed by a post-polymerization deprotection step to reveal the desired functionality. Unfortunately, this protection/deprotection strategy suffers from being: (1) far from “green” and commercially non-viable due to the considerable amount of chemical waste generated, (2) one-dimensional in terms of providing only a single type of functional polyolefin from a single specialized functional monomer, and (3) often deleterious to key thermal phase transition properties, such as the glass transition and melting temperatures,  $T_g$  and  $T_m$ , respectively, due to the functional group typically being incorporated at the end of a flexible alkyl side chain. Finally, it remains a significant challenge to produce symmetric and unsymmetric  $\alpha,\omega$ -difunctionalized (telechelic) polyolefins in programmed fashion, and to the best of our knowledge, telechelic polyolefins that also bear functional groups with orthogonal reactivity within the main chain have never been reported.<sup>[10]</sup> In this regard, we recently introduced a new strategy by which a wide range of telechelic polyolefins can be produced through the LCCTP of olefins using excess equivalents of diphenylzinc ( $\text{ZnPh}_2$ ) as a chain transfer agent (CTA) to incorporate a phenyl group at the start of chain growth, followed by a reactive quench with molecular iodine ( $\text{I}_2$ ) to establish iodo-functionalization at the other chain end.<sup>[11,12]</sup> An optional post-polymerization phenylation reaction can then be used to provide new classes of  $\alpha,\omega$ -bis(phenyl)-terminated polyolefins with programmed differences in tacticity. Importantly, the terminal phenyl group in these new polyolefins can serve as a synthon for various functionalities that are ‘unmasked’ through high-yielding aromatic substitution reactions.<sup>[13]</sup> Herein, we now validate extension of this strategy through the programmed production of multivariate, hyperdimensional functionalized polyolefins of general structure **I** in Scheme 1 in which orthogonally distinguished aryl groups can be positioned at both the end groups and within the main chain. As further summarized in Scheme 1, this strategy relies on the use of cyclopentadienyl, amidinate (CPAM) group 4 metal pre-initiators **1**, which upon “activation” with the borate co-initiator **B1**, express different degrees of stereocontrol over 1-alkene complexation and 1,2-MI for the LCP and LCCTP of a large scope of 1-alkenes, and in the present work, with 4-aryl-1,6-heptadienes (**2**) as comonomers that are incorporated into **I**

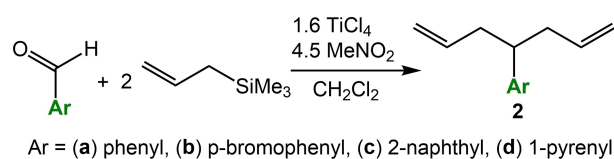


**Scheme 1.** Synthetic route to multivariate, end-group and main-chain functionalized polyolefins via living coordinative chain transfer copolymerization of 1-alkenes and 4-aryl-1,6-heptadienes.

via six-membered-ring cyclopolymerization.<sup>[14,15]</sup> Importantly, the level of incorporation of the main-chain aryl groups in **I** can be easily controlled through manipulation of the comonomer feed ratio, which can optionally be comprised of two or more derivatives of **2** to generate “two- or multi-color” functionalized derivatives of **I**. Alternatively, the living nature of these coordinative co-polymerizations can be harnessed to design and create an unlimited new spectrum of (telechelic) polyolefin microphase-segregated and “color-coded” block copolymers in which each block domain can be selectively functionalized with various levels of incorporation of different aryl groups. Finally, high-yielding post-polymerization processes involving these aromatic substituents can be used to incorporate various new types of reactive functionalities. Collectively, the present results serve to provide access to an even greater hyperdimensional landscape for polyolefin structure and properties that can then form the basis for new science and technology.

To begin, syntheses of the 4-aryl-1,6-heptadienes, where Ar = phenyl (**2a**), *p*-bromophenyl (**2b**), 2-naphthyl (**2c**), and 1-pyrenyl (**2d**), were performed in high yield according to the general published procedure for titanium tetrachloride ( $\text{TiCl}_4$ )-mediated bis-allylation of benzaldehyde according to Scheme 2.<sup>[14a,16,17]</sup> It should be noted that this initial collection of derivatives for **2** was targeted for preliminary investigations only, and it does not imply any limitations of the general methodology. Indeed, further extensions of the strategies presented herein are currently in progress and the results of which will be reported in due course.

Table 1 presents a summary of the results obtained for living coordinative copolymerization of the set of 1-alkenes, defined by 1-hexene (H), 4-methyl-1-pentene (4M1P), propene (P) and 1,5-hexadiene (HXD), and **2a–d** that were



**Scheme 2.** One-step synthesis of 4-aryl-1,6-heptadienes.

**Table 1:** Copolymers **I** obtained by LCP and LCCTP according to Scheme 1.<sup>[a]</sup>

Run	M <sup>[b]</sup> [equiv] <sup>[c]</sup>	<b>2</b> [equiv] <sup>[c]</sup>	<b>1</b>	CTA [equiv] <sup>[c]</sup>	<b>2</b> <sup>[e]</sup> [mol %]	Yield [g]	Yield [%]	M <sub>n</sub> <sup>[f]</sup> [kDa]	<i>D</i> <sup>[f]</sup>	T <sub>g</sub> <sup>[g]</sup> [°C]	T <sub>m</sub> <sup>[g]</sup> [°C]
1	H (180)	<b>2a</b> (20)	<b>1a</b>	0	9.2	0.31	84	23.3	1.68	−30	–
2	H (180)	<b>2a</b> (20)	<b>1b</b>	0	7.7	0.34	92	32.9	1.64	−4	–
3	4M1P (594)	<b>2a</b> (6)	<b>1a</b>	0	1.2	1.01	99	88.5	1.60	38	214/219
4	4M1P (594)	<b>2a</b> (31)	<b>1a</b>	0	4.2	1.06	96	88.0	1.98	43	184/194
5	4M1P (594)	<b>2a</b> (66)	<b>1a</b>	0	9.6	1.14	93	80.0	1.88	45	155
6	P (nd) <sup>[d]</sup>	<b>2a</b> (5)	<b>1a</b>	0	1.2	0.16	n.d.	23.0	1.28	−4	101
7	H (180)	<b>2b</b> (20)	<b>1b</b>	0	9.8	0.37	92	26.2	1.51	−19	–
8	HXD (180)	<b>2b</b> (20)	<b>1b</b>	0	9.7	0.36	90	22.4	1.79	24	–
9	H (180)	<b>2c</b> (20)	<b>1b</b>	0	10.5	0.38	97	22.8	1.51	−1	–
10	H (180)	<b>2d</b> (20)	<b>1b</b>	0	8.5	0.40	94	27.0	1.50	−8	–
11	4M1P (600)	<b>2d</b> (6)	<b>1b</b>	0	0.9	4.72	91	60.1	1.69	34	–
12	H (180)	<b>2a</b> (30), <b>2c</b> (15)	<b>1b</b>	0	18.0	0.42	90	27.0	1.61	6	–
13	H (50), HXD (100)	<b>2a</b> (3)	<b>1b</b>	0	1.9	0.69	89	30.7	1.70	−8	101
14	H (106), HXD (81)	<b>2a</b> (2)	<b>1b</b>	0	3.2	0.75	77	27.5	1.82	−35, 17	–
15	H (297)	<b>2a</b> (15)	<b>1b</b>	ZnEt <sub>2</sub> (5)	4.0	0.50	91	1.1	1.26	−61	–
16 <sup>h</sup>	H (237)	<b>2b</b> (15)	<b>1b</b>	ZnPh <sub>2</sub> (5)	5.6	0.39	83	0.9	1.25	−44	–

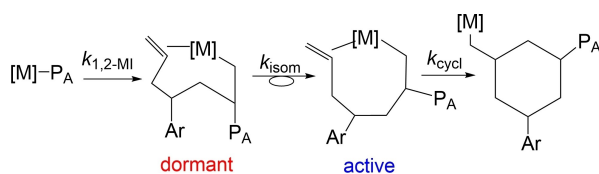
[a] For details of polymerization conditions for each run, see Supporting Information. [b] H=1-hexene, 4M1P=4-methyl-1-pentene, P=propene, HXD=1,5-hexadiene. [c] Relative to **1**. [d] Gaseous monomer held constant at 5 psi. [e] Determined by <sup>1</sup>H NMR. [f] Determined by SEC using polystyrene standards (THF, 40 °C). [g] Determined by DSC. [h] LCCTP was quenched with excess equivalents of I<sub>2</sub>.

conducted according to the general process outlined in Scheme 1 and in either the absence ( $x=0$ ) (LCP) or presence ( $x>0$ ) (LCCTP) of excess equivalents, relative to the active initiator, of a diorganozinc reagent, ZnY<sub>2</sub> (Y=Et or Ph), serving as a CTA.<sup>[3a,8,11]</sup> Different tacticities for **I** were further targeted for production through the selective use of the two different derivatives of **1** as pre-initiators that are activated upon addition of a slight excess of **B1** that serves as co-initiator through protonolysis of a single methyl group.<sup>[7]</sup> More specifically, as we have extensively reported previously, chiral (but racemic) C<sub>1</sub>-symmetric **1a** provides a highly stereoregular isotactic microstructure for the polyolefin product, while achiral C<sub>2</sub>-symmetric **1b** provides an atactic microstructure in the absence of any stereocontrol effected by the growing polymer chain. Finally, excess equivalents of either diethylzinc (ZnEt<sub>2</sub>) or ZnPh<sub>2</sub> as a CTA were employed to establish the functional identity of one end-group of the main chain (e.g. Y=Et or Ph, respectively, in Scheme 1), and then LCCTP was optionally quenched using either an excess of I<sub>2</sub> or a simple protic workup to establish, at the other end of the chain of **I**, either an iodo-terminated (X=I) or unfunctionalized (X=H) end group, respectively.<sup>[8,11,18]</sup>

We have previously reported that the LCP and LCCTP of 1,5-hexadiene and 1,6-heptadiene provides the respective poly(methylene-1,3-cyclopentane) (PMCP) and poly(methylene-1,3-cyclohexane) (PMCH) homopolymers through transition-metal-mediated cyclopolymerization that proceeds through initial 1,2-MI of one alkene moiety of the diene monomer, followed by ring-closing insertion involving the other terminal alkene group.<sup>[7c,i,j,l]</sup> In the case of 1,6-heptadiene, the active propagating species stereospecifically provides a *cis*-1,3-cyclohexane configuration in the repeat units that are then linked together in either isotactic or atactic fashion in the case of **1a** and **1b** as pre-initiators, respectively.<sup>[7i]</sup> This preference for forming a methylene-*cis*-

1,3-cyclohexane moiety was also shown to be preserved for the LCCTP copolymerization of different feed ratios of 1,5-hexadiene/1,6-heptadiene that yielded a new category of poly(methylene-1,3-cyclopentane-*stat*-cyclohexane) statistical copolymers in which the glass transition temperature can be systematically varied from −16 °C to 100 °C as a function of increasing six-membered ring content.<sup>[7j]</sup> In the present work, the living coordinative copolymerization of **2** with different 1-alkenes now introduces a new variable for polymer tacticity in terms of the two different stereochemical outcomes, *syn* and *anti*, that are possible for the 4-aryl substituent relative to the *cis*-1,3-configuration of the six-membered ring within the repeat unit.<sup>[15]</sup>

Copolymer microstructural analyses of all the new grades of **I** of Table 1 using <sup>1</sup>H and <sup>13</sup>C{<sup>1</sup>H} NMR [800 MHz and 200 MHz, respectively, 1,1,2,2-tetrachloroethane-*d*<sub>2</sub> (TCE-*d*<sub>2</sub>), 110 °C] spectroscopy provided strong support for the living nature of each of the LCP and LCCTP processes through the absence of vinylidene resonances that could potentially arise through termination via β-hydrogen atom transfer from the growing polymer chain. Runs 1 and 2 confirmed that both pre-initiators **1a** and **1b** are equally effective for the LCP of **2a** with 1-hexene as comonomers. However higher than expected *D* values were obtained for the polyolefin products of all runs, vis-à-vis *D* typically being <1.1 in the absence of the 4-aryl-1,6-heptadiene comonomers.<sup>[7,8]</sup> Broader dispersity values for a living polymerization are consistent with a propagation mechanism in which a dormant intermediate is kinetically formed and that must undergo a reversible or irreversible degenerate conversion to an active species before further chain growth can occur. Under these conditions, dispersity will be proportional to the rate constant of this process relative to that of propagation.<sup>[19]</sup> As presented in Scheme 3, we speculate that 1,2-MI of **2** initially produces a kinetically dormant intermediate that cannot directly engage in subsequent ring-



**Scheme 3.** Proposed degenerate living coordinative co-polymerization proceeding through kinetic dormant state.

closing cyclization, but that must first undergo conformational reconfiguration to a structure that is now active for this propagation step. Further investigations of the validity of this mechanistic hypothesis are underway.

Runs 3–5 of Table 1 and Figure 2 present results obtained for copolymers of **1** in which 4M1P and **2a** served as the co-monomers. The  $^1\text{H}$  NMR spectra of Figure 2a established that the experimentally realized ratios for incorporation of the two types of repeat units are very close to those expected based on the initial comonomer feed [cf. for run 3 (exp. vs. theor.): 1.2 vs. 1.0, run 4: 4.2 vs. 5.0, and run 5: 9.6 vs. 10.0]. This close agreement is also supportive of a copolymer chain architecture in which the 4-aryl-substituted cyclohexane structural units are randomly distributed and isolated from each other. We have not yet investigated polyolefin products obtained at low polymerization conversion or with much higher amounts of **2** in the comonomer feed ratio, and so it is possible that, in these cases, slight differences in reactivity ratios of the two comonomers could lead to much larger deviations from expectations for either the level or randomness of incorporation of the repeat unit from the 4-aryl-1,6-heptadiene comonomer. The size exclusion chromatography (SEC) data of Figure 2b provide additional confirmation that incorporation of the diene comonomer occurs continuously throughout the living copolymerization and that the relative absorption intensity of the aromatic chromophore observed with the UV/Vis detector tracks accordingly to the overall

SEC profile as obtained with the refractive index (RI) detector. As expected by using **1a** as the pre-initiator, stereochemical microstructural analyses by  $^{13}\text{C}\{^1\text{H}\}$  NMR of the three copolymers of runs 3–5 that are shown in Figure 2c reveal that propagation proceeded in an isoselective fashion with a high degree of stereoregularity as evidenced by the four sharp resonances observed for the mostly isotactic poly(4-methyl-1-pentene) (iPMP) material of run 3. Very interestingly, however, as the level of six-membered ring incorporation increases, there appears to be a corresponding impact on polymer chain stiffness that results in unusually long  $T_1$  times for the two methyl groups ( $\text{C}_5$  and  $\text{C}_6$ ) of the pendant isobutyl group that manifests as a distorted truncated profile for the resonance at 23 ppm. It is possible that this increase in chain stiffness, which also appears as an increase in  $T_g$  values (see Figure 2d) is due to a “sergeant-sailor” mechanism in which an isolated six-membered-ring repeat unit initiates and enforces a long-range helical structure over a length of several iPMP repeat units.<sup>[20]</sup> Although quantitative stereochemical microstructural analyses of tacticity are beyond the scope of the present work, by comparison with the  $^{13}\text{C}\{^1\text{H}\}$  NMR spectra for the homopolymers of iPMP and isotactic *cis*-1,3 PMCH, we further posit that incorporation of **2a** has occurred in a highly stereoselective manner through 1,3-*cis* cyclohexane ring formation, and with the relative configuration of the 4-phenyl substituent being predominantly *anti* to the ring conjunctures. Finally, as the differential scanning calorimetry (DSC) data of Figure 2d reveal, incorporation of an increasing level of methylene-4-phenyl-*cis*-1,3-cyclohexane repeat units within the highly stereoregular iPMP polymer chain microstructure, which can be denoted as *mmmmmmmm* at the *nonad* level, qualitatively has the same effect on  $T_m$  values as that of an increasing level of incorporation of *r* stereocenters, where *m* and *r* signify *meso* and *racemic* (*rac*) relative dyad configurations of two adjacent repeat units, respectively.<sup>[7k]</sup>

Runs 6–9 of Table 1 provide a summary of results obtained for new grades of **1** that are derived from different

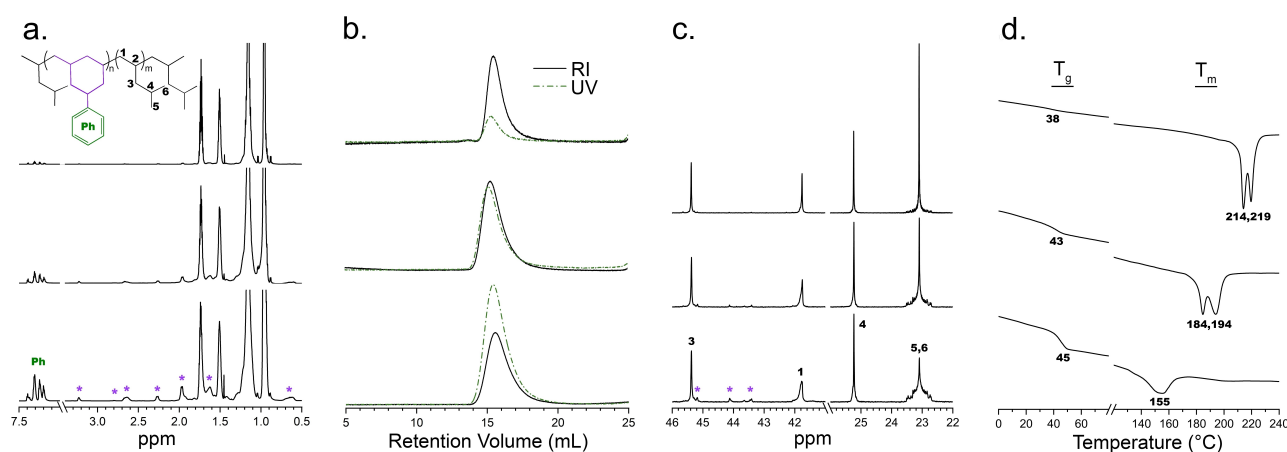


**Figure 2.** a) Partial  $^1\text{H}$  (800 MHz,  $\text{TCE-d}_2$ , 110  $^\circ\text{C}$ ) NMR spectra obtained according to runs 3, 4, and 5 (top to bottom) where purple asterisks denote backbone protons from comonomer **2a**, b) SEC traces with RI and UV detection for the same samples, c) partial  $^{13}\text{C}\{^1\text{H}\}$  (200 MHz,  $\text{TCE-d}_2$ , 110  $^\circ\text{C}$ ) NMR spectra for the same samples where purple asterisks denote backbone carbons from comonomer **2a** and d) partial DSC traces of the second heating cycle measured at 20  $^\circ\text{C}/\text{min}$  for the same samples with bold numbers indicating measured  $T_g$  and  $T_m$  values.



combinations of 1-alkene and **2** as co-monomers.<sup>[15]</sup> As with runs 1–5, the experimentally determined level of incorporation of **2** was often slightly lower than that expected, but this variable could nonetheless be tuned by making appropriate adjustments to the initial feed ratio. Finally, Figure 3 provides comparisons of the absorption (UV/Vis) and emission (fluorescence) electronic spectra for different sets of these new derivatives of **1**. Thus, in Figure 3a, an overlay comparison of the UV/Vis spectra for a constant solution concentration ( $\text{mg mL}^{-1}$ ) of the 4M1P/**2a** copolymer products from runs 3–5 in tetrahydrofuran (THF) shows the expected increase in absorptions by the phenyl group that also remain unperturbed as the level of incorporation of this chromophore increases. Importantly, an overlay of the absorption spectra obtained for the copolymer of run 5 after each of five consecutive dissolution and reprecipitation processes shows no loss of phenyl group concentration (see Figure S92), thereby demonstrating the superiority of using a chemical tether to secure incorporation of fluorescent molecules vis-à-vis previously used physical absorption methods. A similar overlay comparison of the UV/Vis spectra for a series of H/**2** copolymers of **1** in which the identity of the aryl group changes from phenyl (run 2) to 4-bromophenyl (run 7) to 2-naphthyl (run 9) to 1-pyrenyl (run 10) reveal the ability to systematically manipulate

spectral absorption properties of these polyolefins. Very interestingly, even at very low levels of incorporation of the comonomer **2d**, copolymers of **1** are highly fluorescent due to emission from the 1-pyrenyl group. Figure 3c establishes that this property can be incorporated into a transparent mouldable thermoplastic based on the atactic poly(4-methyl-1-pentene) (aPMP)/**2d** copolymer from run 11 in which a 0.9% level of incorporation of **2d** has been achieved, and for which the fluorescence spectrum shown in Figure 3d is strongly indicative of solution emission arising from isolated pyrenyl chromophores. We are now undertaking more detailed investigations of the photophysical properties of the different derivatives of **1** from Table 1. Additionally, run 12 of Table 1 provides preliminary results that validate the strategy of producing “two-color”, and even “multi-color”, grades of **1** in which two or more derivatives of **2** are simultaneously employed as comonomers with 1-alkenes.

Given the living nature of the coordinative co-polymerizations using pre-initiator **1** with different 1-alkene/**2** comonomer combinations, it is possible to design and produce a large range of polyolefin block copolymers (BCPs) in which the optical chromophore of **2** can be selectively located within different block domains. Figure 4 presents a summary of data obtained in pursuit of the validation of this strategy by using our prior reports of the immiscibility of poly(1-hexene) (PH) and PMCP domains within well-defined PMCP-*b*-PH block copolymers that undergo microphase segregation to produce a variety of nanostructured mesophases.<sup>[7b]</sup> In brief, according to run 13 in Table 1, a PMCP-*b*-[PH/**2a**] block copolymer of **1** was produced by sequential LCP of 1,5-hexadiene followed by a comonomer feed of H/**2a** (2 mol %). Figure 4a presents the

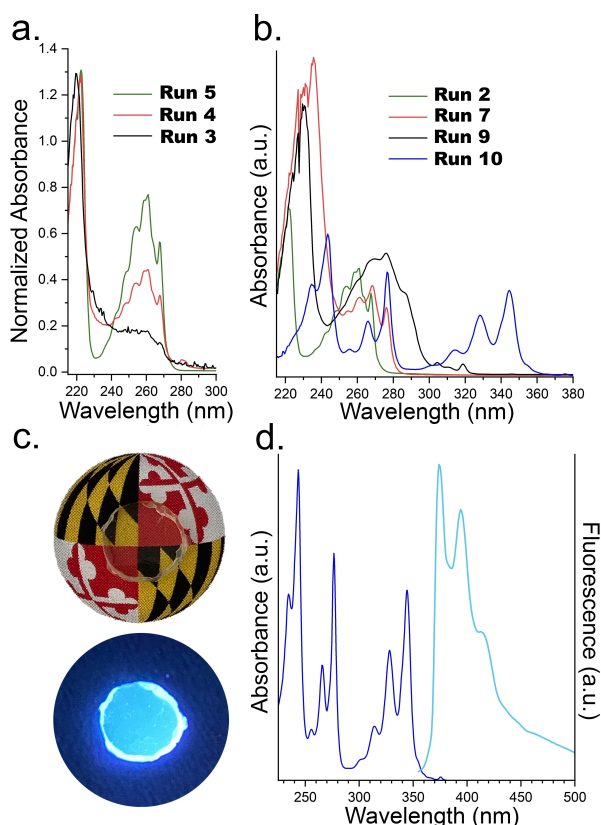


**Figure 3.** Partial UV/Vis spectra of a) runs 3, 4, and 5, b) runs 2, 7, 9, and 10, c) solvent-cast disk of run 11 [7.5 mm (dia.) × 1.0 mm (tk)] under natural light (top) and UV light ( $\lambda_{\text{excitation}} = 254 \text{ nm}$ ) (bottom) and d) absorbance (blue) and fluorescence ( $\lambda_{\text{excitation}} = 344 \text{ nm}$ ) (cyan) spectra of run 11.

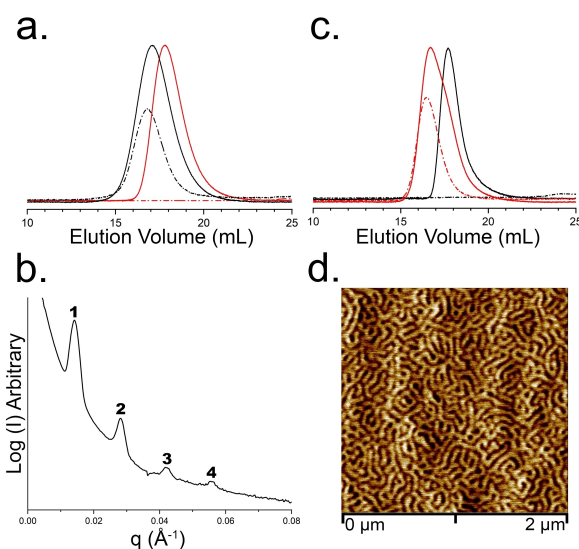


**Figure 4.** a) SEC trace (RI = solid line, UV = dotted line) of run 13 for the first PMCP LCP (red) and the final PMCP-*b*-[PH/**2a**] BCP (black), b) 1D SAXS profile of the LAM phase of run 13 BCP obtained at 125 °C ( $d = 44.5 \text{ nm}$ ), c) SEC trace of run 14 for the first PH LCP (black) and the final PH-*b*-[PMCP/**2a**] BCP (red), d) ps-tm AFM phase map of 30-nm-thick film annealed to 60 °C of run 14 BCP on a carbon-coated Si (c-Si) substrate.

SEC traces for an aliquot taken after formation of the PMCP block (red) and of the final BCP product (black) that serve to confirm that the phenyl group is located only within the PH domain, with a 1.9 % level of incorporation of **2a** as determined by  $^1\text{H}$  NMR analysis. Thermotropic annealing of the bulk material at  $125^\circ\text{C}$  produced a microphase-segregated lamellar (*LAM*) mesophase with a domain spacing of 44.5 nm for this PMCP-*b*-[PH/**2a**] block copolymer as determined by small-angle x-ray scattering (SAXS) characterization data shown in Figure 4b.<sup>[21]</sup> A *LAM* morphology is consistent with the experimentally determined weight fraction of the PMCP domain,  $f_{\text{PMCP}}$ , of 0.53. On the other hand, run 8 of Table 1 confirmed that **2a** can also be incorporated within the PMCP domain of a PMCP-*b*-PH block copolymer. Thus, as demonstrated by run 14 in Table 1, sequential LCP of **1** followed by a 1,5-hexadiene/**2a** (3.0 mol %) comonomer feed was now used to produce the alternative [PMCP/**2a**]-*b*-PH BCP in which the phenyl group, with a 3.2 % level of incorporation, is now located only within the PMCP block domain, as revealed by comparison of the SEC traces shown in Figure 4c. In this case, an experimentally determined  $f_{\text{PMCP}}$  value of 0.44 was determined. The phase map obtained from phase-sensitive tapping mode atomic force microscopy (ps-tm AFM) characterization of an ultra-thin film (thickness = 30 nm) of this [PMCP/**2a**]-*b*-PH BCP, supported on a carbon-coated polycrystalline Si (c-Si) substrate and after thermal annealing at  $60^\circ\text{C}$  for 18 h, presents a “finger-print” surface pattern that is consistent with either a *LAM*<sub>⊥</sub> morphology, in which the alternating lamellar domains are oriented perpendicular to the substrate surface, or a hexagonal cylindrical mesophase, *HEX*<sub>||</sub>, in which the cylindrical domains are oriented parallel with the substrate.<sup>[7b,j,11b]</sup> A domain spacing of 75.0 nm that is obtained from this phase map can only be viewed as the upper limit value due to non-deconvolution of spatial effects of the probe tip. Finally, while additional SAXS characterization of this block copolymer conclusively shows the absence of a pure *LAM* morphology, only a mixed *LAM*/*HEX* mesophase can be tentatively assigned due to possible molar mass dispersity effects and the lack of long range periodic ordering.<sup>[16,22]</sup> Clearly, though, based on these preliminary results, it is not hard to envision a much broader range of additional BCP designs in which block domains can be “color-coded” by using sequential additions of different 1-alkene/**2** combinations.

As a final consideration, runs 15 and 16 of Table 1 provide preliminary results obtained from an investigation of the ability of **2** to function as a comonomer along with 1-alkenes for LCCTP in which excess equivalents of  $\text{ZnEt}_2$  or  $\text{ZnPh}_2$  are used as CTAs. Most notably, run 16 presents the LCCTP of a H/**2b** comonomer feed with  $\text{ZnPh}_2$  as the CTA that was then terminated by the addition of excess equivalents of  $\text{I}_2$  to produce the unique unsymmetric telechelic copolymer shown in Figure 5 in which the aryl groups at one terminus and within the main-chain are structurally different and with orthogonal reactivity towards post-polymerization reactions, such as aromatic electrophilic substitution and transition-metal-catalyzed Negishi coupling. It is important to note that, at the level of incorporation of

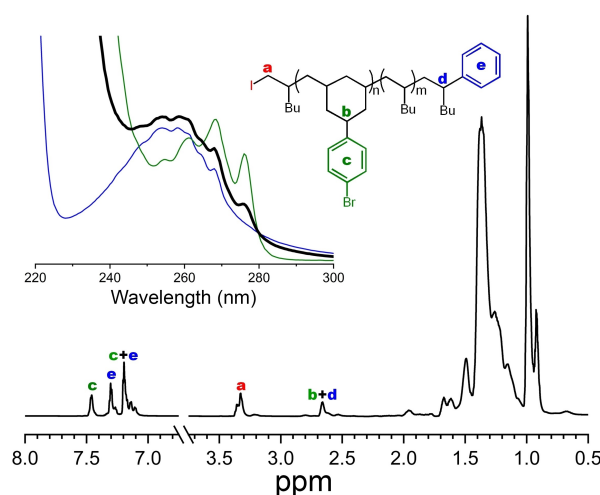


**Figure 5.** Partial  $^1\text{H}$  (800 MHz,  $\text{TCE-d}_2$ ,  $90^\circ\text{C}$ ) NMR spectrum of the telechelic copolymer from run 16. Inset provides an overlay comparison of the UV/Vis spectrum (with arbitrary absorbance as y-axis) for the copolymer product of run 16 (black), run 8 (green), and an independently synthesized I-aPH-Ph standard<sup>[11a]</sup> (blue).

**2b**, we are not able to distinguish and quantify by NMR the possible alternative occurrence of an iodo-end group arising from quenching of LCP with this comonomer as the terminal repeat unit, and accordingly, only the iodo-end group due to iodine quench after 1-hexene insertion is shown in Figure 5. The use of this and other dual functionalized telechelic variants of derivative of **1** as building blocks for the design of novel polyolefin-based materials is now a wide-open landscape that can deliver new discoveries, new science, and new technologies.

In summary, the past 70 years have witnessed incredible advances with the development of new catalysts, polymerization mechanisms, and reactor designs that have served to greatly expand the structures and properties of purely hydrocarbon-based polyolefins. The present results now serve to throw the door wide open to many different dimensional levels of telechelic and main-chain functionalized polyolefins that can be both designed and obtained in practical and scalable quantities for the purpose of moving beyond simple *functionalized* polyolefins to the greater challenge of crafting and utilizing *functional* polyolefins.

## Experimental Section

Complete experimental details are provided in the Supporting Information.

## Author Contributions

D.M.F and K.A.K. performed experimental work and L.R.S supervised the project. All authors contributed to the analysis, Figures, and writing of the manuscript.

## Acknowledgements

Support of this work was provided by grants from the National Science Foundation (NSF) (CHE-1955730 and 2247554) and the National Institute of Standards and Technology (NIST) (70NANB21H112) to L.R.S. for which he is grateful. Funding for the AFM shared facility used in this research was provided by NSF (CHE-1626288).

## Conflict of Interest

The corresponding author has a financial interest in the university spin-out company, Precision Polyolefins, LLC (PPL). This work did not involve any PPL personnel, funding, or other resources and all new intellectual property has been disclosed in accordance with state and federal requirements.

## Data Availability Statement

The data that support the findings of this study are available from the corresponding author upon reasonable request.

**Keywords:** Functional · Living Polymerization · Polyolefin

- [1] a) G. Natta, P. Pino, P. Corradini, F. Danusso, E. Mantica, G. Mazzanti, G. Moraglio, *J. Am. Chem. Soc.* **1955**, *77*, 1708–1710; b) G. Natta, *Atti Accad. Naz. Lincei Mem.* **1955**, *4*, 61; c) P. Corradini, *J. Polym. Sci. Part A* **2004**, *42*, 391–395.
- [2] a) *Handbook of Polyolefins* (Ed.: C. Vasile), Marcel Dekker, New York, **2000**; b) “Polyolefins: 50 years after Ziegler and Natta I: Polyethylene and Polypropylene”: *Advances in Polymer Science*, Vol. 257 (Ed.: W. Kaminsky), Springer, Heidelberg, **2013**; c) “Polyolefins: 50 years after Ziegler and Natta II: Polyolefins by Metallocenes and Other Single-Site Catalysts”: *Advances in Polymer Science*, Vol. 258 (Ed.: W. Kaminsky), Springer, Heidelberg, **2013**; d) *Polyolefin Compounds and Materials* (Eds.: M. Al-AliAlMa'adeed, I. Krupa), Springer, Heidelberg, **2016**.
- [3] For relevant reviews of “next generation” polyolefins, see: a) L. R. Sita, *Angew. Chem. Int. Ed.* **2009**, *48*, 2464–2472; b) P. D. Hustad, *Science* **2009**, *325*, 704–707; c) M. Stürzel, S. Mihan, R. Mülhaupt, *Chem. Rev.* **2016**, *116*, 1398–1433; d) T. Kida, R. Tanaka, Y. Hiejima, K. Nitta, T. Shiono, *Polymer* **2021**, *218*, 123526; e) T. V. Tran, L. H. Doi, *Eur. Polym. J.* **2021**, *142*, 110100; f) G. Zanchin, G. Leone, *Prog. Polym. Sci.* **2021**, *113*, 101342.
- [4] a) L. Forni, R. Invernizzi, *Ind. Eng. Chem. Process Des. Dev.* **1973**, *12*, 455–459; b) Y. Suzuki, T. Yasumoto, K. Mashima, J. Okuda, *J. Am. Chem. Soc.* **2006**, *128*, 13017–13025; c) O. L. Sydora, *Organometallics* **2019**, *38*, 997–1010; d) H. Jin, H. Jiang, S. Yang, G. He, X. Guo, *Chem. Eng. Commun.* **2019**, *206*, 346–354.
- [5] *Stereoselective Polymerization with Single-Site Catalysts* (Eds.: L. S. Baugh, J. M. Canich), CRC, Boca Raton, **2008**.
- [6] G. J. Domski, J. M. Rose, G. W. Coates, A. D. Bolig, M. Brookhart, *Prog. Polym. Sci.* **2007**, *32*, 30–92.
- [7] For leading references of the LCP of  $\alpha$ -olefins and  $\alpha,\omega$ -nonconjugated dienes related to the goals of the present work, see: a) K. C. Jayaratne, L. R. Sita, *J. Am. Chem. Soc.* **2000**, *122*, 958–959; b) K. C. Jayaratne, R. J. Keaton, D. A. Henningsen, L. R. Sita, *J. Am. Chem. Soc.* **2000**, *122*, 10490–10491; c) K. C. Jayaratne, L. R. Sita, *J. Am. Chem. Soc.* **2001**, *123*, 10754–10755; d) R. J. Keaton, K. C. Jayaratne, D. A. Henningsen, L. A. Koterwas, L. R. Sita, *J. Am. Chem. Soc.* **2001**, *123*, 6197–6198; e) Y. Zhang, R. J. Keaton, L. R. Sita, *J. Am. Chem. Soc.* **2003**, *125*, 9062–9069; f) Y. Zhang, L. R. Sita, *J. Am. Chem. Soc.* **2004**, *126*, 7776–7777; g) M. B. Harney, Y. Zhang, L. R. Sita, *Angew. Chem. Int. Ed.* **2006**, *45*, 6140–6144; h) W. Zhang, L. R. Sita, *Adv. Synth. Catal.* **2008**, *350*, 439–447; i) C. Giller, G. Gururajan, J. Wei, W. Zhang, W. Hwang, D. B. Chase, J. F. Rabolt, L. R. Sita, *Macromolecules* **2011**, *44*, 471–482; j) K. E. Crawford, L. R. Sita, *J. Am. Chem. Soc.* **2013**, *135*, 8778–8781; k) K. E. Crawford, L. R. Sita, *ACS Macro Lett.* **2015**, *4*, 921–925; l) C. M. Wentz, D. M. Fischbach, L. R. Sita, *Angew. Chem. Int. Ed.* **2022**, *61*, e202211992; m) W. R. Burgenson, C. M. Wentz, L. R. Sita, *ACS Macro Lett.* **2023**, *12*, 101–106.
- [8] For leading references on LCCTP of olefins and  $\alpha,\omega$ -nonconjugated dienes related to the goals of the present work, see: a) W. Zhang, L. R. Sita, *J. Am. Chem. Soc.* **2008**, *130*, 442–443; b) W. Zhang, J. Wei, L. R. Sita, *Macromolecules* **2008**, *41*, 7829–7833; c) M. A. Wallace, P. Y. Zavalij, L. R. Sita, *ACS Catal.* **2020**, *10*, 8496–8502; d) M. A. Wallace, C. M. Wentz, L. R. Sita, *ACS Catal.* **2021**, *11*, 4583–4592; e) M. A. Wallace, L. R. Sita, *ACS Catal.* **2021**, *11*, 9754–9760; f) M. A. Wallace, L. R. Sita, *Angew. Chem. Int. Ed.* **2021**, *60*, 19671–19678.
- [9] a) L. Oliva, P. Longo, L. Izzo, M. Di Serio, *Macromolecules* **1997**, *30*, 5616–5619; b) T. C. Chung, G. Xu, Y. Lu, Y. Hu, *Macromolecules* **2001**, *34*, 8040–8050; c) K. Hakala, T. Helaja, B. Löfgren, *Polym. Bull.* **2001**, *46*, 123–130; d) E. Drent, R. van Dijk, R. van Ginkel, B. van Oort, R. I. Pugh, *Chem. Commun.* **2002**, 744–745; e) J.-F. Lahitte, F. Peruch, S. Plentz-Meneghetti, F. Isel, P. J. Lutz, *Macromol. Chem. Phys.* **2003**, *203*, 2583–2589; f) J.-Y. Dong, Y. Hu, *Coord. Chem. Rev.* **2006**, *250*, 47–65; g) H. Makio, T. Fujita, *Macromol. Rapid Commun.* **2007**, *28*, 698–703; h) Y. Zheng, Y. Li, L. Pan, Y. Li, *Polymer* **2007**, *48*, 2496–2502; i) Y. Zheng, L. Pan, Y.-G. Li, Y.-S. Li, *Eur. Polym. J.* **2008**, *44*, 475–482; j) A.-S. Rodrigues, J.-F. Carpentier, *Coord. Chem. Rev.* **2008**, *252*, 2137–2154; k) D. Takeuchi, R. Matsuura, Y. Fukuda, K. Osakada, *Dalton Trans.* **2009**, *41*, 8955–8962; l) N. M. G. Franssen, J. N. H. Reek, B. de Bruin, *Chem. Soc. Rev.* **2013**, *42*, 5809–5832; m) M. Jaymand, *Polym. Chem.* **2014**, *5*, 2663–2690; n) B. P. Carrow, K. Nozaki, *Macromolecules* **2014**, *47*, 2541–2555; o) C. Wang, G. Luo, M. Nishiura, G. Song, A. Yamamoto, Y. Li, Z. Hou, *Sci. Adv.* **2017**, *3*, e1701011; p) M. Bouyahyi, Y. Turki, A. Tanwar, L. Jasinska-Walc, R. Duchateau, *ACS Catal.* **2019**, *9*, 7779–7790; q) X. Hu, X. Ma, Z. Jian, *Polym. Chem.* **2019**, *10*, 1912–1919; r) J. Chen, Y. Gao, T. J. Marks, *Angew. Chem. Int. Ed.* **2020**, *59*, 14726–14735; s) S. Onbulak, M. A. Hillmyer, *Polym. Chem.* **2021**, *12*, 1681–1691; t) L. Jasinska-Walc, M. Bouyahyi, R. Duchateau, *Acc. Chem. Res.* **2022**, *55*, 1985–1996; u) Z. Balzade, F. Sharif, S. R. Ghaffarian Anbaran, *Macromolecules* **2022**, *55*, 6938–6972; v) Y. Zhao, H. Li, S. Xin, H. Li, Y. Luo, S. He, *Organometallics* **2022**, *41*, 3514–3521; w) Z. Zhang, Y. Jiang, R. Lei, Y. Zhang, S. Li, D. Cui, *Macromolecules* **2023**, *56*, 2476–2483.
- [10] For a recent review of telechelic polyolefins, see: T. Yan, D. Guironnet, *Polym. Chem.* **2021**, *12*, 5126–5138.
- [11] a) M. A. Wallace, A. A. Burkey, L. R. Sita, *ACS Catal.* **2021**, *11*, 10170–10178; b) A. A. Burkey, D. M. Fischbach, C. M. Wentz, K. L. Beers, L. R. Sita, *ACS Macro Lett.* **2022**, *11*, 402–409; c) B. R. S. Kuzminski, D. M. Fischbach, G. P. A. Yap, L. R. Sita, *Organometallics* **2022**, *41*, 3122–3127.
- [12] R. Briquel, J. Mazzolini, T. Le Bris, O. Boyron, F. Boisson, F. Delolme, F. D'Agosto, C. Boisson, R. Spitz, *Angew. Chem. Int. Ed.* **2008**, *47*, 9311–9313.

- [13] Friedel–Crafts acylation of polystyrene has previously been used to incorporate functional groups, see, for instance: a) M. Biswas, S. Chatterjee, *Angew. Makromol. Chem.* **1983**, *113*, 11–19; b) M. Biswas, S. Chatterjee, *Eur. Polym. J.* **1983**, *19*, 317–320; c) D. S. Argyropoulos, H. I. Bolker, *Makromol. Chem.* **1986**, *187*, 1887–1894; d) B. Hird, A. Eisenberg, *J. Polym. Sci. Part A* **1993**, *31*, 1377–1381; e) J. Li, H.-M. Li, *Eur. Polym. J.* **2005**, *41*, 823–829; f) Y. Chen, A. E. Tavakley, T. M. Mathias, T. A. Taton, *J. Polym. Sci. Part A* **2006**, *44*, 2604–2614; g) Y. Gao, H. Li, X. Wang, *Eur. Polym. J.* **2007**, *43*, 1258–1266; h) G. Liu, Y. Guan, Y. Ge, L. Xie, *J. Appl. Polym. Sci.* **2011**, *120*, 3278–3283; i) F. Liu, S. Chen, Y. Gao, Y. Xie, *J. Appl. Polym. Sci.* **2017**, *134*, 45046.
- [14] Ring-opening polymerization of 4-phenyl-1-cyclopentene, which is obtained from 4-phenyl-1,6-heptadiene through ring-closing metathesis, has been previously used to prepare a polypentenamer in which phenyl groups are positioned at every fifth carbon atom, and after hydrogenation, aromatic sulfonation has been used to produce a main-chain functionalized polyolefin material, see: a) W. J. Neary, J. G. Kennemur, *Macromol. Rapid Commun.* **2016**, *37*, 975–979; b) R. J. Kieber III, W. J. Neary, J. G. Kennemur, *Ind. Eng. Chem. Res.* **2018**, *57*, 4916–4922; c) A. Kendrick IV, W. J. Neary, J. D. Delgado, M. Bohlmann, J. G. Kennemur, *Macromol. Rapid Commun.* **2018**, *39*, 1800145.
- [15] It has been reported that the non-living coordination homopolymerization of 4-phenyl-1,6-heptadiene by a chiral  $C_2$ -symmetric *ansa*-bridged bis(tetrahydroindenyl)zirconocene/methylaluminoxane (MAO) catalyst combination produces a poly(methylene-4-phenyl-1,2-cyclopentane) chain structure, see: D. Takeuchi, R. Matsura, Y. Fukuda, K. Osakada, *Dalton Trans.* **2009**, 8955–8962.
- [16] Experimental details are provided in the Supporting Information.
- [17] A.-C. Durand, L. Brahmi, M. Lahrech, S. Hacini, M. Santelli, *Synth. Commun.* **2005**, *35*, 1825–1833.
- [18] a) T. S. Thomas, W. Hwang, L. R. Sita, *Angew. Chem. Int. Ed.* **2016**, *55*, 4683–4687; b) S. R. Nowak, W. Hwang, L. R. Sita, *J. Am. Chem. Soc.* **2017**, *139*, 5281–5284; c) K. K. Lachmayr, C. M. Wentz, L. R. Sita, *Angew. Chem. Int. Ed.* **2020**, *59*, 1521–1526; d) K. K. Lachmayr, L. R. Sita, *Angew. Chem. Int. Ed.* **2020**, *59*, 3563–3567; e) S. R. Nowak, K. K. Lachmayr, K. G. Yager, L. R. Sita, *Angew. Chem. Int. Ed.* **2021**, *60*, 8710–8716.
- [19] A. H. E. Müller, R. Zhuang, D. Yan, G. Litvinenko, *Macromolecules* **1995**, *28*, 4326–4333.
- [20] a) A. Nuermaimaiti, C. Bombis, M. M. Knudsen, J. R. Cramer, E. Laegsgaard, F. Besenbacher, K. V. Gothelf, T. R. Linderoth, *ACS Nano* **2014**, *8*, 8074–8081; b) K. Cobos, R. Rodríguez, E. Quiñoñ, R. Riguera, F. Freire, *Angew. Chem. Int. Ed.* **2020**, *59*, 23724–23730.
- [21] a) O. Glatter, O. Kratky *Small Angle X-ray Scattering*, Academic Press, New York, **1982**; b) I. W. Hamley, V. Castelletto, *Prog. Polym. Sci.* **2004**, *29*, 909–948.
- [22] a) N. A. Lynd, A. J. Meuler, M. A. Hillmyer, *Prog. Polym. Sci.* **2008**, *33*, 875–893; b) D. T. Gentekos, B. P. Fors, *ACS Macro Lett.* **2018**, *7*, 677–682; c) D. T. Gentekos, J. Jia, E. S. Tirado, K. P. Barteau, D. M. Smilgies, R. A. DiStasio, Jr., B. P. Fors, *J. Am. Chem. Soc.* **2018**, *140*, 4639–4648; d) L. M. Pitet, B. M. Chamberlain, A. W. Hauser, M. A. Hillmyer, *Polym. Chem.* **2019**, *10*, 5385–5395.

Manuscript received: April 3, 2023

Accepted manuscript online: May 30, 2023

Version of record online: May 30, 2023